From 1D Chain to 3D Network: Syntheses, Structures, and Properties of $K_2MnSn_2Se_6$, $K_2MnSnSe_4$, and $K_2Ag_2SnSe_4$

Xuean Chen,[†] Xiaoying Huang,[†] Aihua Fu,[†] Jing Li,*[,†] Li-Dan Zhang,[‡] and Hong-You Guo[‡]

Department of Chemistry, Rutgers University, Camden, New Jersey 08102, and Department of Applied Chemistry, Beijing University of Chemical Technology, Beijing, 100029, P. R. China

Received January 20, 2000. Revised Manuscript Received May 15, 2000

$K_2MnSn_2Se_6$ (**I**), $K_2MnSnSe_4$ (**II**), and $K_2Ag_2SnSe_4$ (**III**) were prepared by molten-salt (alkali-metal polyselenide flux) reactions at intermediate temperature (400−520 °C). Their crystal structures were determined by single-crystal X-ray diffraction techniques. Crystal data for **I**: space group $P4/ncc$, $a = 8.167(1)$, $c = 19.724(4)$ Å, $Z = 4$, $R1/wR2 = 0.0435/0.0722$ for 592 observed reflections and 29 variables; crystal data for **II**: space group $P\bar{4}n2$, $a = 10.574(1)$, $c = 8.301(2)$ Å, $Z = 2$, $R1/wR2 = 0.0339/0.0939$ for 1208 observed reflections and 40 parameters; crystal data for **III**: space group $P2/c$, $a = 7.575(2)$, $b = 5.920(1)$, $c = 12.148(2)$ Å, $\beta = 113.56(3)°$, $Z = 2$, $R1/wR2 = 0.0595/0.1135$ for 1098 observed reflections and 45 parameters. The crystal structure of **I** consists of infinite $^1_\infty[MnSn_2Se_6]^{2-}$ anionic chains containing $[Sn_2Se_6^{4-}]$ units linked by tetrahedrally coordinated Mn^{2+} ions, with the K^+ cations situated between the chains. **II** contains a three-dimensional framework formed by corner- and edge-sharing $SnSe_4$ and $MnSe_4$ tetrahedra, with large channels hosting the K^+ cations. **III** is a layered compound containing $^2_\infty[Ag_2SnSe_4]^{2-}$ anionic layers separated by K^+ counterions. The anionic layer is formed by parallel SiS_2-type $^1_\infty[AgSe_2]^{3-}$ chains cross-linked by tetrahedral $SnSe_4$ via bridging selenium atoms of the chains. The results from differential scanning calorimetry (DSC) measurements show that **I** is stable up to 590 °C, **II** decomposes at about 243 °C, and **III** melts congruently at about 510 °C. **I**, **II**, and **III** are semiconductors with estimated band gaps of 2.0, 1.7, and 1.8 eV, respectively.

Introduction

A number of quaternary alkali-transition metal chalcogenostannates with crystal formula of $A_2T_lM_mQ_n$ (A = alkali metal, T = transition or post-transition metal, M = main-group metal, Q = S, Se, Te; l, $m = 1, 2$; $n = 4, 6$) have been recently prepared employing the molten alkali-metal polychalcogenide flux technique. These compounds possess a variety of structure types ranging from one dimensional (1D) to three dimensional (3D) and are characterized by incorporating $[SnQ_4]^{4-}$ or $[Sn_2Q_6]^{4-}$ (Q = S, Se, and Te) as basic building-blocks. For example, compounds $A_2Cu_2Sn_2Q_6$ (A = Na, K, Rb, Cs, Q = S; A = K, Rb, Q = Se) display $^1_\infty[SnQ_3]^{2-}$ ribbons built upon corner-sharing $[SnQ_4]^{4-}$ tetrahedra, which are further linked together by two terminal Q atoms through strongly distorted CuQ_4 tetrahedra into two-dimensional (2D) sheets.[1] The 1D $^1_\infty[SnQ_3]^{2-}$ ribbons have also been observed in a series of compounds such as $K_2MnSn_2S_6$, $Cs_2MnSn_2S_6$, and $Rb_2ZnSn_2S_6$.[2] On the other hand, $Rb_2Cu_2SnS_4$ contains a row of $[SnS_4]^{4-}$ tetrahedra that are connected by Cu atoms to generate a layer structure;[1] $K_2Au_2SnS_4$ contains parallel $^1_\infty[Au_2SnS_4]^{2-}$ zigzag chains which are constructed by tetrahedral $[SnS_4]^{4-}$ and linear $[AuS_2]^{3-}$ building-blocks in a ratio of 1:2;[1] $K_2Au_2Sn_2Q_6$ (Q = S, Se) is also a 1D compound, however, its anionic chains contain dimeric $[Sn_2Q_6]^{4-}$ units linked by linear-coordinated Au^+ ions;[1,3] $K_2Ag_2SnTe_4$, reported by us previously, contains a 3D porous framework generated by linking $[SnTe_4]^{4-}$ tetrahedra to Ag atoms, with large channels hosting the K^+ cations.[4]

In this paper, we report the preparation, crystal structures, and optical and thermal properties of three new members of this class of compounds: $K_2MnSn_2Se_6$ (**I**), $K_2MnSnSe_4$ (**II**), and $K_2Ag_2SnSe_4$ (**III**). Among them, structure **I** represents another example in which Zintl anion $[Sn_2Se_6]^{4-}$ acts as a building-block to bridge transition metal centers into infinite chains; structure **II** contains $SnSe_4$ tetrahedra which share corners and edges with $MnSe_4$ tetrahedra to result in a 3D network; and the crystal structure of **III** is a 2D layered type closely related to $Rb_2Cu_2SnS_4$ structure.

Experimental Section

Materials. K_2Se was prepared by reactions of potassium metal and elemental selenium in a 2:1 ratio in liquid ammonia,

* To whom correspondence should be addressed.
[†] Rutgers University.
[‡] Beijing University of Chemical Technology.

(1) Liao, J.-H.; Kanatzidis, M. G. *Chem. Mater.* **1993**, *5*, 1561−1569.
(2) Kanatzidis, M. G.; Sutorik, A. C. *Prog. Inorg. Chem.* **1995**, *43*, 151−265.
(3) Löken, S.; Tremel, W. *Z. Anorg. Allg. Chem.* **1998**, *624*, 1588−1594.
(4) Li, J.; Guo, H.-Y.; Proserpio, D. M.; Sironi, A. *J. Solid State Chem.* **1995**, *117*, 247−255.

10.1021/cm0000447 CCC: $19.00
Published on Web 07/18/2000

Table 1. Crystallographic Data for $K_2MnSn_2Se_6$ (I), $K_2MnSnSe_4$ (II), and $K_2Ag_2SnSe_4$ (III)

	I	II	III
formula	$K_2MnSn_2Se_6$	$K_2MnSnSe_4$	$K_2Ag_2SnSe_4$
formula weight	844.28	567.67	728.47
crystal size, mm	0.22 × 0.15 × 0.04	0.20 × 0.13 × 0.10	0.12 × 0.12 × 0.01
space group	*P*4/*ncc* (no. 130)	$P\bar{4}n2$ (no. 118)	*P*2/*c* (no. 13)
a, Å	8.167(1)	10.574(1)	7.575(2)
b, Å	8.167(1)	10.574(1)	5.920(1)
c, Å	19.724(4)	8.301(2)	12.148(2)
α, deg	90	90	90
β, deg	90	90	113.56(3)
γ, deg	90	90	90
V, Å^3, *Z*	1315.8(4), 4	928.1(3), 2	499.4(2), 2
d_{calc}, g/cm^3	4.262	4.063	4.845
λ, Å	0.71073	0.71073	0.71073
μ, mm^{-1}	21.888	20.545	21.696
$2\theta_{max}$, deg	60	60	60
total reflections	3562	1432	1527
unique reflections	971	1352	1436
observed [$I \geq 2\sigma(I)$]	592	1208	1098
no. of variables	29	40	45
GOF[a] on F_o^2	1.234	1.331	1.667
R indices [$I \geq 2\sigma(I)$]	*R*1[b] 0.0435	0.0339	0.0595
*wR*2[c] 0.0722	0.0939	0.1135	
R indices (all data)	*R*1 0.0765	0.0463	0.0814
*wR*2 0.0823	0.0968	0.1186	

[a] $GOF = \sqrt{\sum[w(F_o^2-F_c^2)^2]/n-p}$. [b] $R1 = \sum||F_o| - |F_c||/\sum|F_o|$. [c] $wR2 = \sqrt{\sum[w(F_o^2-F_c^2)^2]/\sum w(F_o^2)^2}$..

and SnSe was prepared by a stoichiometric reaction of elements at 450 °C. The other chemicals were used as purchased without further treatment. These included K (99.5%, Strem Chemicals, Inc.), Mn (99%, Aldrich Chemical Co.), Ag (99.9%, Aldrich Chemical Co.), Sn (99.9%, Fisher Scientific), and Se (99.5%, Strem Chemicals, Inc.).

Synthesis. For the preparation of $K_2MnSn_2Se_6$ (**I**), 0.080 g (0.5 mmol) K_2Se, 0.027 g (0.5 mmol) Mn, 0.198 g (1.0 mmol) SnSe, and 0.118 g (1.5 mmol) Se were weighed in a glovebox under an atmosphere of argon. The mixture was introduced into a thin-walled Pyrex tube and sealed at pressure of ~10^{-3} Torr. The tubes were gradually heated to 520 °C, where they were kept for 4 days, then cooled at a rate of 4 °C/h to 150 °C. The orange-red rectangular platelike crystals were collected in ca. 70% yield after the reaction product was washed with dimethylformamide (DMF) and anhydrous ethanol and dried with anhydrous diethyl ether. Direct reaction of a stoichiometric mixture of elements at 500 °C for 1 week yielded a single-phase polycrystalline sample that was confirmed by powder X-ray analysis.

$K_2MnSnSe_4$ (**II**) was synthesized from a reaction containing 0.054 g (0.34 mmol) K_2Se, 0.010 g (0.18 mmol) Mn, 0.020 g (0.17 mmol) Sn, and 0.106 g (1.36 mmol) Se. The sample was slowly heated to and maintained at 400 °C for 1 week, followed by a slow cooling (4 °C/h) to room temperature. After the excess flux was removed with DMF, red polyhedral-shaped crystals were isolated in about 20% yield.

$K_2Ag_2SnSe_4$ (**III**) was prepared in the same way as **I**, except with a different ratio of the reagents. The reaction mixture contained 0.080 g (0.5 mmol) K_2Se, 0.054 g (0.5 mmol) Ag, 0.030 g (0.25 mmol) Sn, and 0.158 g (2 mmol) Se. The reaction was kept at 500 °C for 1 week. The same isolation procedure as for **I** and **II** was used and red platelike crystals were obtained in high yield (about 90%). All three compounds appear to be relatively stable in air and water.

Crystal Structure Determination. Intensity data of the title compounds were collected at room temperature (293 ± 1°K) on an Enraf-Nonius CAD4 automatic diffractometer with graphite monochromated Mo Kα radiation. Cell dimensions were obtained from a least-squares refinement with 25 automatically centered reflections in the range 6.38° ≤ *θ* ≤ 13.96° (**I**), 7.83° ≤ *θ* ≤ 16.46° (**II**), and 7.42° ≤ *θ* ≤ 15.81° (**III**). Three standard reflections were remeasured every 2 h. No decay was observed except the statistic fluctuation in the range of ±5.6% (**I**), ± 2.6% (**II**), and ±3.0% (**III**). Raw intensities were corrected for Lorentz and polarization effects, and for absorption by empirical method based on *ψ*-scan data. Direct phase determination and subsequent difference Fourier map synthesis yielded the positions of all atoms, all of which were eventually subjected to the anisotropic refinements. An extinction correction was applied to the calculated structure factors and refined to 0.00126(5) (**I**), 0.0169(6) (**II**), and 0.0134(6) (**III**). Because both Mn and Sn occupy tetrahedral sites with similar Mn−Se and Sn−Se distances in **I** and **II**, and the position of Ag in the periodic table lies close to that of Sn, there is a potential for disorder in all three structures. To examine whether Mn and Sn, Ag, and Sn are statistically distributed over the metal sites, occupancy parameters of Mn, Ag, and Sn atoms were allowed to vary along with their positional and thermal parameters during the refinements, while the occupancy parameters of K and Se atoms were fixed at 1.0. The resultant occupancies are 0.98(1) for Sn and 1.00(1) for Mn in **I**, 0.98(2) for Mn2 and 1.03(1) for Sn in **II**, and 0.99(1) for Sn and 1.00(1) for Ag in **III**. These figures are all within standard deviations from the ideal values. Therefore, in the final least-squares cycles, the ordered models with ideal atomic occupancies were assumed. For compound **I**, the final full-matrix least-squares refinements on F^2 lead to $R1 = 0.0435$ and $wR2 = 0.0722$ for 592 observed reflections ($I > 2\sigma(I)$) and 29 variables. The reliability factors for compound **II** (**III**) converged to $R1 = 0.0339$ (0.0595) and $wR2 = 0.0939$ (0.1135) for 1208 (1098) observed reflections, 40 (45) parameters. Refinement of Flack parameter for **II** gave a value of 0.03(3), indicating the absolute structure to be correct. The examination of the positional parameters of **III** did not reveal potential additional symmetry, and the listed largest correlation matrix elements (0.53−0.86) did not apply to any atomic coordinates. The final difference electron density maps showed no features in all cases. Details of crystal parameters, data collection, and structure refinements are given in Table 1. All computations were performed using the SHELX97 program package,[5] and crystal structure drawings were produced with SCHAKAL 92.[6] The final atomic coordinates and the equivalent isotropic displacement parameters are listed in Tables 2, 3, and 4.

Thermal Analysis. Differential scanning calorimetry (DSC) measurements were carried out on a computer-controlled TA

(5) Sheldrick, G. M. *SHELX-97: Program for Structure Refinement*; University of Goettingen: Germany, 1997.

(6) Keller, E. *SCHAKAL 92: A Computer Program for Graphical Representation of Crystallographic Models*; University of Freiburg: Freiburg, Germany, 1992.

Table 2. Atomic Coordinates and Equivalent Isotropic Temperature Factors[a] (Å²) for $K_2MnSn_2Se_6$ (I)

atoms	*X*	*y*	*z*	U_{eq}
Sn	0.75	0.25	0.3374(1)	0.020(1)
Mn	0.75	0.25	0.5	0.021(1)
Se(1)	0.5898(1)	0.4306(1)	0.4152(1)	0.022(1)
Se(2)	0.5861(1)	0.0861(1)	0.25	0.023(1)
K(1)	0.25	0.25	0.4743(2)	0.041(1)
K(2)	0.25	0.25	0.1789(2)	0.036(1)

[a] U_{eq} is defined as one-third of the trace of the orthogonalized **U** tensor.

Table 3. Atomic Coordinates and Equivalent Isotropic Temperature Factors* (Å²) for $K_2MnSnSe_4$ (II)

atoms	*x*	*y*	*z*	U_{eq}
Sn	0.2780(1)	0.2220(1)	0.25	0.016(1)
Mn(1)	0.5	0	0.25	0.022(1)
Mn(2)	0	0	0.5	0.017(1)
Se(1)	0.3026(1)	0.0305(1)	0.0709(1)	0.020(1)
Se(2)	0.0675(1)	0.2144(1)	0.3908(2)	0.023(1)
K(1)	0.2466(3)	0.7466(3)	0.25	0.033(1)
K(2)	0	0.5	0.25	0.023(1)
K(3)	0	0	0	0.049(2)

[a] U_{eq} is defined as one-third of the trace of the orthogonalized **U** tensor.

Table 4. Atomic Coordinates and Equivalent Isotropic Temperature Factors* (Å²) for $K_2Ag_2SnSe_4$ (III)

atoms	*x*	*y*	*z*	U_{eq}
Ag	0.4991(2)	0.2499(2)	0.5331(1)	0.038(1)
Sn	0.5	0.2491(2)	0.25	0.019(1)
Se(1)	0.2672(2)	0.0306(2)	0.3104(1)	0.024(1)
Se(2)	0.2667(2)	0.4701(2)	0.0746(1)	0.023(1)
K(1)	0	0.5228(8)	0.25	0.035(1)
K(2)	0	0	0	0.037(1)

[a] U_{eq} is defined as one-third of the trace of the orthogonalized **U** tensor.

Instrument DSC-2920 analyzer. Powder samples of **I** (14.120 mg), **II** (7.750 mg), and **III** (11.100 mg) were sealed into aluminum pans. An approximately equal mass of sealed empty aluminum pan was used as a reference. The samples were heated at a rate of 5 °C/min from room temperature to 590 °C and then cooled under nitrogen gas current. The residues were examined by powder X-ray diffraction immediately after the DSC experiments.

Diffuse Reflectance Measurements. Optical diffuse reflectance spectra were measured at room temperature with a Shimadzu UV-3101PC double-beam, double-monochromator spectrophotometer. Data were collected in the wavelength range 250−2000 nm. $BaSO_4$ powder was used as a standard (100% reflectance). A similar procedure as previously described[7] was used to collect and convert the data using the Kubelka−Munk function.[8] The scattering coefficient (*S*) was treated as a constant because the average particle size of the samples used in the measurements was significantly larger than 5 μm.

Results and Discussion

Structure Description of $K_2MnSn_2Se_6$. $K_2MnSn_2Se_6$ (**I**) crystallizes in a new structure type and it is a 1D compound containing infinite $^1_\infty[MnSn_2Se_6]^{2-}$ chains (Figure 1A). The anionic chains, which are closely related to those found in $KFeS_2$,[9] can be viewed as an ordered version of SiS_2 structure in which manganese and tin atoms occupy the silicon sites, and selenium atoms replace the sulfur positions.[10] The chains propagate along the [001] direction and are well separated by charge balancing K^+ cations, as seen in Figure 1B. Each $^1_\infty[MnSn_2Se_6]^{2-}$ chain consists of edge-sharing $MnSe_4$ and $SnSe_4$ ions (through opposite edges) that alternate in a 1:2 ratio. The Mn^{2+} ion is situated on a crystallographic $\bar{4}$ axis, resulting in the adjacent $[Sn_2Se_6]^{4-}$ units being rotated 90° with respect to each other. As a result, the repeating unit is composed of six edge-sharing tetrahedra (*Sechser* single chains[11]) with a period of 19.724(4) Å (equal to the unit cell *c*-axis). The $MnSe_4$ tetrahedra are distorted, giving two sets of Se−Mn−Se angles, 99.40(3)° and 114.73(2)° (Table 5), with the smaller angle being associated with the constrained Se1−Mn−Se1−Sn four-membered rings. The Mn−Se distance of 2.5853(8) Å compares well with those found in related compounds such as $LiMnSe_2$ (2.555(2)−2.562(8) Å), $NaMnSe_2$ (2.566(2)−2.597(6) Å), and $RbMnSe_2$ (2.569(1) Å),[12] all featuring tetrahedrally coordinated Mn. In the $[Sn_2Se_6]^{4-}$ unit, Sn−Se1 distance (2.4985(8) Å) is about 0.06 Å shorter than Sn−Se2 distance (2.5614(9) Å), which follows the general pattern observed in the isolated dimers[13] that the "terminal" Sn−Se bonds are normally stronger than the corresponding bridge bonds. The only difference is that the Sn_2Se_2 rings in $K_2MnSn_2Se_6$ become more strained as the structure extends from the dimer to a 1D chain upon

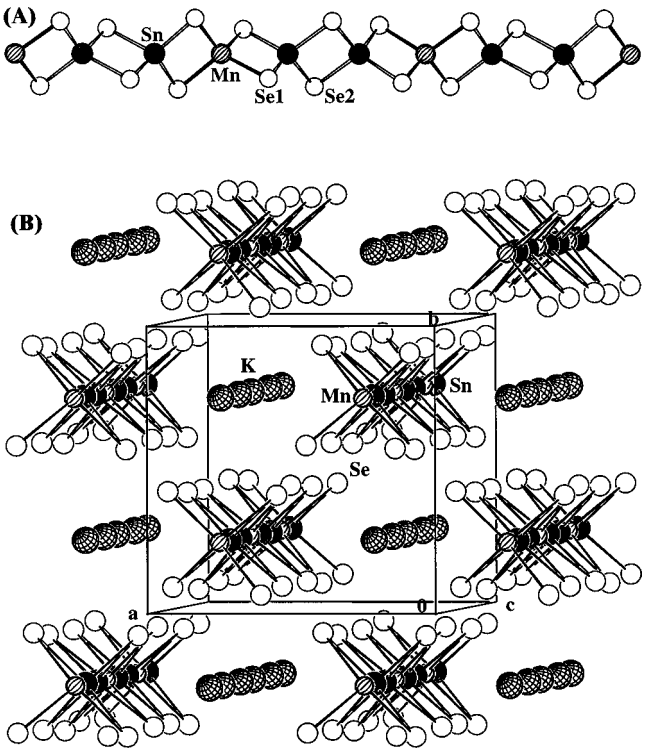

Figure 1. (A) Fragment of the $^1_\infty[MnSn_2Se_6]^{2-}$ anionic chain. (B) Unit cell of $K_2MnSn_2Se_6$ (**I**) projected approximately along the *c*-axis.

(7) Li, J.; Chen, Z.; Wang, X.-X.; Proserpio, D. M. *J. Alloys Compd.* **1997**, *262*−*263*, 28−33.
(8) Wendlandt, W. Wm.; Hecht, H. G. *Reflectance Spectroscopy*; Interscience: A Division of John Wiley & Sons: New York, 1966.
(9) Boon, J. W.; MacGillavry, C. H. *Recl. Trav. Chim. Pays-Bas* **1942**, *61*, 910−920.
(10) Peters, J.; Krebs, B. *Acta Crystallogr.* **1982**, *38*, 1270−1272.
(11) Liebau, F. In *Structural Chemistry of Silicates*; Springer: Berlin, 1985.
(12) Kim, J.; Hughbanks, T. *J. Solid State Chem.* **1999**, *146*, 217−225.
(13) Eisenmann, B.; Hansa, J. *Z. Kristallogr.* **1993**, *203*, 299−300.

Table 5. Selected Bond Lengths (Å) and Angles (deg) for $K_2MnSn_2Se_6$ (I)[a]

Sn−Se(1)^{i}	2.4985(8)	K(1)−Se(1)^{ix}	3.352(2)
Sn−Se(1)	2.4985(8)	K(1)−Se(1)^{v}	3.642(3)
Sn−Se(2)	2.5614(9)	K(1)−Se(1)^{x}	3.642(3)
Sn−Se(2)^{i}	2.5614(9)	K(1)−Se(1)^{iv}	3.642(3)
Mn−Se(1)^{iii}	2.5853(8)	K(1)−Se(1)^{xi}	3.642(3)
Mn−Se(1)^{iv}	2.5853(8)	K(2)−Se(2)	3.361(2)
Mn−Se(1)	2.5853(8)	K(2)−Se(2)^{ix}	3.361(2)
Mn−Se(1)^{i}	2.5853(8)	K(2)−Se(2)^{viii}	3.361(2)
Sn−Sn^{vi}	3.450(1)	K(2)−Se(2)^{vii}	3.361(2)
Sn−Mn	3.2067(9)	K(2)−Se(1)^{xii}	3.458(2)
K(1)−Se(1)	3.352(2)	K(2)−Se(1)^{ii}	3.458(2)
K(1)−Se(1)^{vii}	3.352(2)	K(2)−Se(1)^{xiii}	3.458(2)
K(1)−Se(1)^{viii}	3.352(2)	K(2)−Se(1)^{xiv}	3.458(2)
Se(1)^{i}−Sn−Se(1)	104.22(4)	Se(1)^{iii}−Mn−Se(1)	114.73(2)
Se(1)^{i}−Sn−Se(2)	112.26(2)	Se(1)^{iv}−Mn−Se(1)	114.73(2)
Se(1)−Sn−Se(2)	116.65(2)	Se(1)^{iii}−Mn−Se(1)^{i}	114.73(2)
Se(1)^{i}−Sn−Se(2)^{i}	116.65(2)	Se(1)^{iv}−Mn−Se(1)^{i}	114.73(2)
Se(1)−Sn−Se(2)^{i}	112.26(2)	Se(1)−Mn−Se(1)^{i}	99.40(3)
Se(2)−Sn−Se(2)^{i}	95.33(4)	Sn−Se(1)−Mn	78.19(3)
Se(1)^{iii}−Mn−Se(1)^{iv}	99.40(3)	Sn−Se(2)−Sn^{vi}	84.67(4)

[a] Symmetry codes: (i) $-x+3/2, -y+1/2, z$; (ii) $-x+1, y-1/2, -z+1/2$; (iii) $y+1/2, -x+1, -z+1$; (iv) $-y+1, x-1/2, -z+1$; (v) $-x+1, -y+1, -z+1$; (vi) $y+1/2, x-1/2; -z+1/2$; (vii) $-x+1/2, -y+1/2, z$; (viii) $y, -x+1/2, z$; (ix) $-y+1/2, x, z$; (x) $x-1/2, y-1/2, -z+1$; (xi) $y-1/2, -x+1, -z+1$; (xii) $y-1/2, x-1/2, -z+1/2$; (xiii) $-y+1, -x+1, -z+1/2$; (xiv) $x-1/2, -y+1, -z+1/2$.

insertion of Mn^{2+}. This is reflected by a slight decrease of both Sn···Sn distance and Sn−Se−Sn angle in the ring (e.g., 3.450(1) Å, 84.67(4)° in $K_2MnSn_2Se_6$ vs 3.514(3) Å, 85.53(6)° in $K_4Sn_2Se_6$).[13] There are two crystallographically distinct potassium cations, and each lies on a 4-fold axis and is coordinated by eight Se atoms in a square antiprismatic arrangement. The K−Se distances, 3.352(2)−3.642(3) Å (average 3.453 Å), are in the same range as reported for the eight-coordinated K^+ in $K_2Au_2Sn_2Se_6$ (average 3.477 Å).[3] The shortest interchain Se−Se contact is 3.781(1) Å, eliminating any significant Se−Se bonding interactions.

Structure Description of $K_2MnSnSe_4$. $K_2MnSnSe_4$ (**II**) crystallizes in the noncentrosymmetric space group $P\bar{4}n2$ and it contains $MnSe_4$ and $SnSe_4$ tetrahedra as the basic construction units. The crystal structure is closely related to that of K_2AgSbS_4.[14] In fact, the space group $Pnn2$ of K_2AgSbS_4 is a maximal nonisomorphic subgroup (index 2) of the group $P\bar{4}n2$ adopted by $K_2MnSnSe_4$. The symmetry reduction represents a step that is "*translationengleich*".[15] There are two distinct $MnSe_4$ units, of which Mn1-centered tetrahedra are situated at the *ac* and *bc* planes of the unit cell and four of them are arranged in a tetrahedral geometry, while the Mn2-centered tetrahedra are located at the centers of the *ab* plane as well as at the middle of the cell edges parallel to the *c*-axis (Figure 2). Each Mn1-centered tetrahedron shares two opposite edges with two $SnSe_4$ tetrahedra to form a $MnSn_2Se_8$ structural motif, which is further connected to four tetrahedral Mn2 via its four terminal Se2 atoms (μ_2-ligands). Likewise each Mn2-centered tetrahedron also corner shares with four $MnSn_2Se_8$ units along all directions to give rise to a 3D extended network (see Figures 2 and 3). Alternatively, the 3D network can also be considered to be built upon 2D sheets in the following way (see Figure 3): within

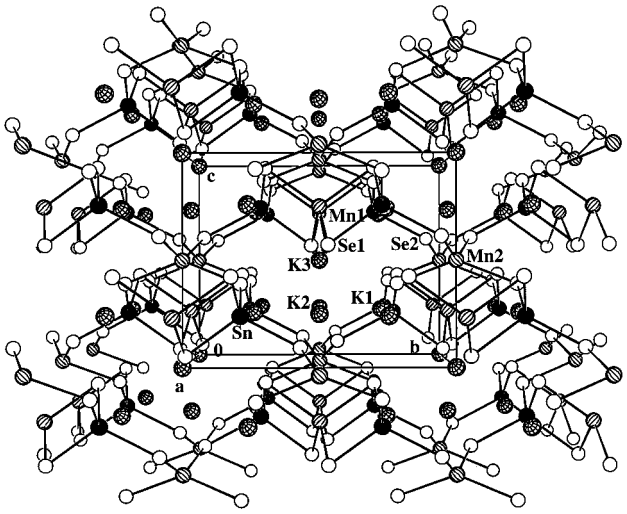

Figure 2. Perspective view of the $K_2MnSnSe_4$ (**II**) structure along the *a*-axis. The channels with the same morphology also run parallel to the *b*-axis.

the *ab* plane, the $Mn1Sn_2Se_8$ and its translationally generated partners are linked together by sharing two vertexes of Mn2-centered tetrahedron to generate a 2D network. Applying the *n*-glide symmetry operations to this layer produces the neighboring equivalent layers along the [001] direction. These layers are then connected to each other by sharing the other two vertexes of each Mn2-centered tetrahedron to form a 3D network. The 3D network contains orthogonal, intersecting open channels running parallel to the [100] and [010] directions (Figure 2). The tunnel has a V-shaped cross section created from the edges of alternating four $SnSe_4$ and four $MnSe_4$ tetrahedra. The K2 and K3 cations reside in the channels, while the K1 cations are located at the pockets between the adjacent $SnSe_4$ tetrahedra, when viewed down the *a*-axis.

Selected bond lengths and angles are given in Table 6. It is clear that the $SnSe_4$ tetrahedra are nearly regular with the bond distances Sn−Se = 2.516(1)−2.525(1) Å and angles Se−Sn−Se = 100.48(6)°−115.63(4)°. The values are in good agreement with those observed in $K_2MnSn_2Se_6$ and $K_2Ag_2SnSe_4$, which will be discussed next. The Mn1 atom is located at the intersecting point of three mutually perpendicular 2-fold rotational axes and the Mn2 atom is situated on a crystallographic $\bar{4}$ axis, which gives rise to a single distance of 2.583(1) Å for Mn1−Se and 2.544(1) Å for Mn2−Se, respectively (Table 6). The Se−Mn−Se bond angles vary from 97.44(5)° to 122.23(5)° (for Mn1) and from 97.30(2)° to 138.24(6)° (for Mn2). The smallest Se−Mn1−Se angle is again associated with the constrained Se1−Mn1−Se1−Sn four-membered rings, whereas the distortion around the Mn2 atom arises because four of its attached $MnSn_2Se_8$ slabs are arranged in a compressed tetrahedral geometry in the direction of the *c*-axis. Of the three independent potassium atoms, K1 and K2 are surrounded by eight Se atoms with normal K−Se distances ranging from 3.316(1) to 3.588(2) Å, while K3 are four coordinate to Se atoms with a single shorter K−Se distance of 3.269(1) Å. The tetracoodinated K^+ are rather rare. Several limited examples include K_2Se (K−Se distances, 3.324 Å),[16] K_5Se_3 (K−Se = 3.214(6)−3.222(5) Å),[17] and K_6MnSe_4 (K−Se = 3.220(4)−3.340(4) Å).[18]

(14) Schimek, G. L.; Pennington, W. T.; Wood, P. T.; Kolis, J. W. *J. Solid State Chem.* **1996**, *123*, 277−284.

(15) *International Tables for X-ray Crystallography*; Kluwer Academic Publishers: Dordrecht, 1989; Vol. C.

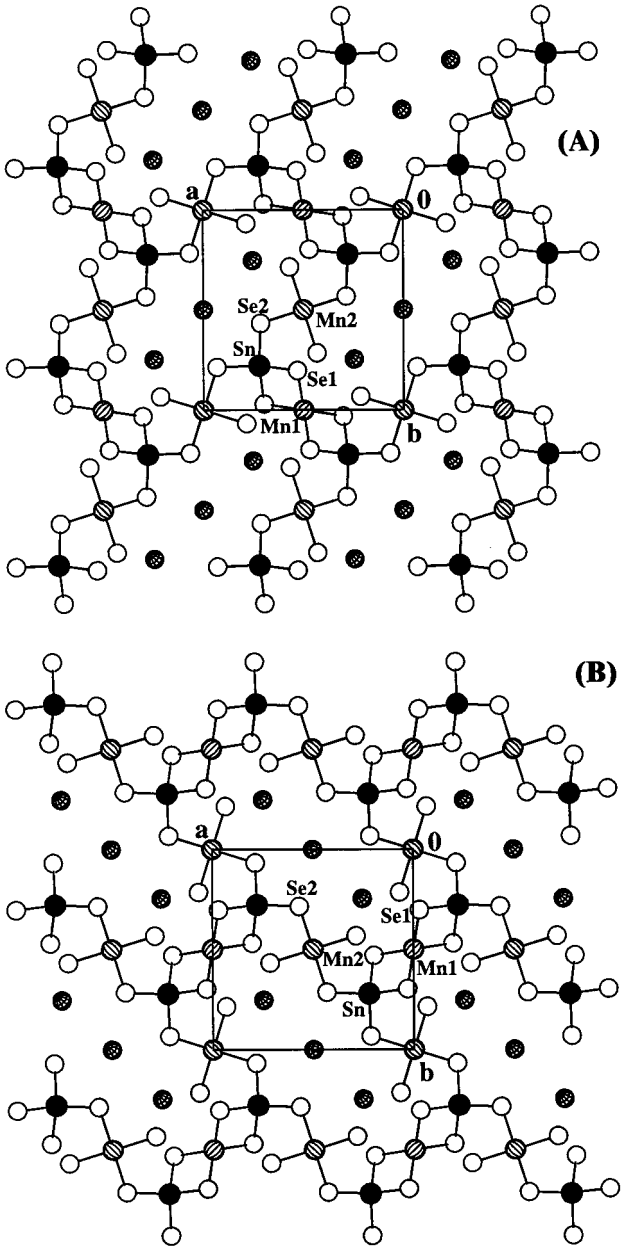

Figure 3. A slice of the anionic framework at (A) $z \sim 1/4$ and (B) $z \sim 3/4$ in $K_2MnSnSe_4$ (**II**).

To the best of our knowledge, no structurally characterized quaternary manganese-containing selenostannates have been reported. Several chemically related thiostannates are $K_2MnSn_2S_6$, $Cs_2MnSn_2S_6$, and K_2MnSnS_4,[2,19] none of which show any direct structural relation to the selenide analogues presented here. The crystal structure of $K_2MnSn_2S_6$, as well as the isotypic $Cs_2MnSn_2S_6$, contain 1D $^1_\infty[SnS_3]^{2-}$ ribbons produced by corner sharing SnS_4 tetrahedra. These ribbons are connected through tetrahedrally coordinated Mn atoms to generate a 3D framework containing six-membered $[MnSn_2S_3]$ rings.[2,19] K_2MnSnS_4 has a quite different assembly in which the statistically distributed Mn and Sn atoms form the $[Mn_2Sn_2S_{10}]^{8-}$ adamantane-like units that are subsequently linked together through their four terminal S atoms to yield 2D sheets of $^2_\infty[Mn_2Sn_2S_8]^{4-}$.[2] Our attempts to prepare the Cs analogue $Cs_2MnSn_2Se_6$ have so far been unsuccessful.

Table 6. Selected Bond Lengths (Å) and Angles (deg) for $K_2MnSnSe_4$ (II)[a]

Sn−Se(2)^{i}	2.516(1)	K(1)−Se(1)^{xi}	3.548(3)
Sn−Se(2)	2.516(1)	K(1)−Se(1)^{xii}	3.548(3)
Sn−Se(1)	2.525(1)	K(1)−Se(2)^{xiii}	3.588(2)
Sn−Se(1)^{i}	2.525(1)	K(1)−Se(2)^{xiv}	3.588(2)
Mn(1)−Se(1)	2.583(1)	K(2)−Se(2)	3.316(1)
Mn(1)−Se(1)^{i}	2.583(1)	K(2)−Se(2)^{xv}	3.316(1)
Mn(1)−Se(1)^{ii}	2.583(1)	K(2)−Se(2)^{viii}	3.316(1)
Mn(1)−Se(1)^{iii}	2.583(1)	K(2)−Se(2)^{i}	3.316(1)
Mn(2)−Se(2)^{iv}	2.544(1)	K(2)−Se(1)^{xii}	3.399(1)
Mn(2)−Se(2)	2.544(1)	K(2)−Se(1)^{xvi}	3.399(1)
Mn(2)−Se(2)^{v}	2.544(1)	K(2)−Se(1)^{xi}	3.399(1)
Mn(2)−Se(2)^{vi}	2.544(1)	K(2)−Se(1)^{xvii}	3.399(1)
Sn−Mn(1)	3.319(1)	K(3)−Se(1)	3.269(1)
K(1)−Se(1)^{ix}	3.402(3)	K(3)−Se(1)^{vii}	3.269(1)
K(1)−Se(1)^{x}	3.402(3)	K(3)−Se(1)^{iv}	3.269(1)
K(1)−Se(2)^{i}	3.545(3)	K(3)−Se(1)^{xvi}	3.269(1)
K(1)−Se(2)^{viii}	3.545(3)		
Se(2)^{i}−Sn−Se(2)	105.79(6)	Se(1)^{i}−Mn(1)−Se(1)^{iii}	109.71(5)
Se(2)^{i}−Sn−Se(1)	115.63(4)	Se(1)^{ii}−Mn(1)−Se(1)^{iii}	97.44(5)
Se(2)−Sn−Se(1)	109.82(4)	Se(2)^{iv}−Mn(2)−Se(2)	138.24(6)
Se(2)^{i}−Sn−Se(1)^{i}	109.82(4)	Se(2)^{iv}−Mn(2)−Se(2)^{v}	97.30(2)
Se(2)−Sn−Se(1)^{i}	115.63(4)	Se(2)−Mn(2)−Se(2)^{v}	97.30(2)
Se(1)−Sn−Se(1)^{i}	100.48(6)	Se(2)^{iv}−Mn(2)−Se(2)^{vi}	97.30(2)
Se(1)−Mn(1)−Se(1)^{i}	97.44(5)	Se(2)−Mn(2)−Se(2)^{vi}	97.30(2)
Se(1)−Mn(1)−Se(1)^{ii}	109.71(5)	Se(2)^{v}−Mn(2)−Se(2)^{vi}	138.24(6)
Se(1)^{i}−Mn(1)−Se(1)^{ii}	122.23(5)	Sn−Se(1)−Mn(1)	81.04(4)
Se(1)−Mn(1)−Se(1)^{iii}	122.23(5)	Sn−Se(2)−Mn(2)	116.24(5)

[a] Symmetry codes: (i) $-y + 1/2, -x + 1/2, -z + 1/2$; (ii) $-x + 1, -y, z$; (iii) $y + 1/2, x - 1/2, -z + 1/2$; (iv) $-x, -y, z$; (v) $y, -x, -z + 1$; (vi) $-y, x, -z + 1$; (vii) $y, -x, -z$; (viii) $-x, -y + 1, z$; (ix) $y + 1/2, x + 1/2, -z + 1/2$; (x) $x, y + 1, z$; (xi) $y, -x + 1, -z$; (xii) $-x + 1/2, y + 1/2, z + 1/2$; (xiii) $y, -x + 1, -z + 1$; (xiv) $-x + 1/2, y + 1/2, z - 1/2$; (xv) $y - 1/2, x + 1/2, -z + 1/2$; (xvi) $-y, x, -z$; (xvii) $x - 1/2, -y + 1/2, z + 1/2$.

Structure Description of $K_2Ag_2SnSe_4$. $K_2Ag_2SnSe_4$ is a layered compound containing infinite 2D $^2_\infty[Ag_2SnSe_4]^{2-}$ anionic layers separated by K^+ counterions (Figure 4A). The anionic layer, which is isostructural to the $^2_\infty[Cu_2SnS_4]^{2-}$ framework in $Rb_2Cu_2SnS_4$,[1] can be described as containing SiS_2-type of $^1_\infty[AgSe_2]^{3-}$ 1D chains generated by edge sharing of the $AgSe_4$ tetrahedra. These chains run parallel to the *b*-axis and are cross-linked by tetrahedral $SnSe_4$ via μ_3-bridging selenium atoms of the $^1_\infty[AgSe_2]^{3-}$ chains to result in a 2D layer. Because Sn occupies only one-half of the available tetrahedral sites, the layer is formed with one-quarter of the tetrahedral voids unoccupied (Figure 4B). The crystal structure of $K_2Ag_2SnSe_4$ may also be described as a monoclinic variant of the $Rb_2Cu_2SnS_4$-type. A group-subgroup relationship between the two structures can be rationalized by means of a "Bärnighausen tree",[20] which is illustrated in Scheme 1. The indices of the *translationengleiche* (t) and *klassengleiche* (k) transitions, as well as the unit cell transformations, are given in the scheme. A comparison of the atomic parameters demonstrates that the Ag and Sn positions in $K_2Ag_2SnSe_4$ remain close to those of the Cu and Sn atoms in $Rb_2Cu_2SnS_4$, whereas the alkali metal and chalcogen sites show significant displacements. For instance, the Rb^+ cations in $Rb_2Cu_2SnS_4$ are eight

(16) Zintl, E.; Harder, A.; Dauth, B. *Z. Elektrochemie* **1934**, *40*, 588−593.
(17) Schewe-Miller, I.; Boettcher, P. *Z. Kristallographie* **1991**, *196*, 137−151.
(18) Bronger, W.; Balk-Hardtdegen, H. *Z. Anorg. Allg. Chem.* **1989**, *574*, 89−98.
(19) Sheldrick, W. S.; Wachhold, M. *Coord. Chem. Rev.* **1998**, *176*, 211−322.
(20) Bärnighausen, H. *Commun. Math. Chem.* **1980**, *9*, 139−175.

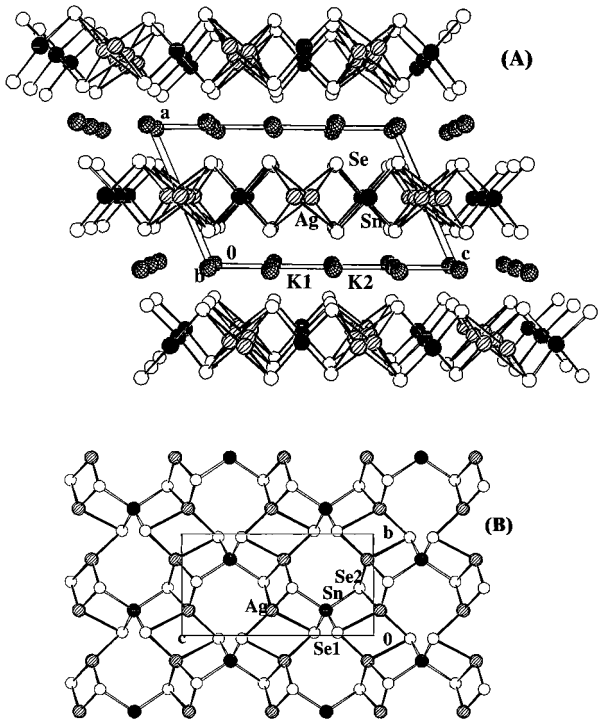

Figure 4. (A) Perspective view of the $K_2Ag_2SnSe_4$ (**III**) structure along the [010] direction. (B) Projection of the $^2_\infty[Ag_2SnSe_4]^{2-}$ anionic layer along the monoclinic [100] direction.

Scheme 1

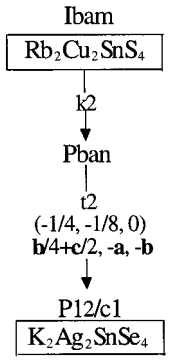

coordinate to sulfur atoms, in a nearly regular square prismatic geometry, with Rb−S and S−S distances falling in a narrow range of 3.411(8)−3.522(8) Å and 3.844−4.194 Å, respectively,[1] whereas in $K_2Ag_2SnSe_4$ the corresponding K−Se (Se−Se) distances are wider: 3.455(4)−3.642(2) Å (3.713(3)−4.382(2) Å) for the K1 site, and 3.344(1)−3.644(1) Å (3.713(3)−4.382(2) Å) for the K2 site (Table 7). We believe that the replacement of Rb^+ by the smaller K^+, and replacement of S^{2-} by the larger Se^{2-} results in a significant distortion of the coordination environments around the alkali metal cations, which in turn causes a lowering of the space-group symmetry going from $Rb_2Cu_2SnS_4$ to $K_2Ag_2SnSe_4$. The observed X-ray powder diffraction patterns of $K_2Ag_2SnSe_4$ were in good agreement with those calculated from the single-crystal data. The weak lines such as those at $2\theta = 16.00°$ and 24.19° that were absent in the theoretical X-ray diffraction (XRD) patterns of the orthorhombic $Rb_2Cu_2SnS_4$-type structure confirmed the monoclinic symmetry. Although Ag and Sn atoms are anticipated to be crystallographically difficult to discern,

Table 7. Selected Bond Lengths (Å) and Angles (deg) for $K_2Ag_2SnSe_4$ (III)[a]

Ag−Se(2)^{i}	2.610(2)	K(1)−Se(2)^{v}	3.487(2)
Ag−Se(1)^{ii}	2.611(2)	K(1)−Se(1)^{x}	3.534(4)
Ag−Se(1)	2.880(2)	K(1)−Se(1)^{xi}	3.534(4)
Ag−Se(2)^{iii}	2.901(2)	K(1)−Se(2)^{i}	3.642(2)
Sn−Se(1)	2.521(1)	K(1)−Se(2)^{ix}	3.642(2)
Sn−Se(1)^{iii}	2.521(1)	K(2)−Se(2)	3.344(1)
Sn−Se(2)^{iii}	2.523(2)	K(2)−Se(2)^{xiv}	3.344(1)
Sn−Se(2)	2.523(2)	K(2)−Se(1)	3.499(2)
Ag−Ag^{ii}	3.068(3)	K(2)−Se(1)^{xiv}	3.499(2)
Ag−Ag^{iv}	3.069(3)	K(2)−Se(1)^{xv}	3.628(1)
Ag−Sn	3.441(1)	K(2)−Se(1)^{v}	3.628(1)
K(1)−Se(1)	3.455(4)	K(2)−Se(2)^{ix}	3.644(1)
K(1)−Se(1)^{v}	3.455(4)	K(2)−Se(2)^{vii}	3.644(1)
K(1)−Se(2)	3.487(2)		
Se(2)^{i}−Ag−Se(1)^{ii}	125.19(6)	Se(1)−Sn−Se(2)	100.16(4)
Se(2)^{i}−Ag−Se(1)	105.22(6)	Se(1)^{iii}−Sn−Se(2)	110.85(4)
Se(1)^{ii}−Ag−Se(1)	112.27(6)	Se(2)^{iii}−Sn−Se(2)	117.52(8)
Se(2)^{i}−Ag−Se(2)^{iii}	112.54(5)	Sn−Se(1)−Ag^{ii}	100.88(6)
Se(1)^{ii}−Ag−Se(2)^{iii}	104.81(6)	Sn−Se(1)−Ag	78.86(5)
Se(1)−Ag−Se(2)^{iii}	91.86(5)	Ag^{ii}−Se(1)−Ag	67.73(6)
Se(1)−Sn−Se(1)^{iii}	118.25(8)	Sn−Se(2)−Ag^{viii}	101.16(6)
Se(1)−Sn−Se(2)^{iii}	110.85(4)	Sn−Se(2)−Ag^{iii}	78.43(5)
Se(1)^{iii}−Sn−Se(2)^{iii}	100.16(4)	Ag^{viii}−Se(2)−Ag^{iii}	67.46(5)

[a] Symmetry codes: (i) $x, -y+1, z+1/2$; (ii) $-x+1, -y, -z+1$; (iii) $-x+1, y, -z+1/2$; (iv) $-x+1, -y+1, -z+1$; (v) $-x, y, -z+1/2$; (vi) $x+1, y, z$; (vii) $x, y-1, z$; (viii) $x, -y+1, z-1/2$; (ix) $-x, -y+1, -z$; (x) $x, y+1, z$; (xi) $-x, y+1, -z+1/2$; (xii) $x-1, -y+1, z-1/2$; (xiii) $x-1, y, z$; (xiv) $-x, -y, -z$; (xv) $x, -y, z-1/2$.

the $K_2Ag_2SnSe_4$ case is an exception. There are two independent tetrahedral metal sites (4g and 2f) within the unit cell. The assignment of these sites to silver and tin atoms, respectively, was based on the electron count that gave a reasonable, charge balanced formula and was in good agreement with the corresponding interatomic distances. This structural model was supported by structural refinements which led to relatively high atomic displacement parameters of the Ag atoms (Table 4) as well as the relatively short Ag···Ag contacts (3.068(3) Å, compared to Ag···Sn of 3.441(1) Å), characteristic of d^{10} cations. Notice that the silver atoms form a zigzag chain (Figure 4B), suggesting that the compound may be ionic conducting at high temperature.

Table 7 lists the selected atomic distances and angles. As can be seen, the tetrahedral environments around tin atoms are almost regular, with the Se−Sn−Se angles being very close to the value of a perfect tetrahedron. The Sn−Se bond lengths vary from 2.521(1) to 2.523(2) Å, comparable with those found in $K_2MnSn_2Se_6$ and $K_2MnSnSe_4$. In contrast, the $AgSe_4$ tetrahedra are severely distorted, with Ag−Se distances divided into two sets. A set of two shortest Ag−Se contacts (2.610(2), 2.611(2) Å) forms the largest Se−Ag−Se angles (125.19(6)°), whereas another set of two longest Ag−Se contacts (2.880(2), 2.901(2) Å) has the smallest bond angle of 91.86(5)°. Other Se−Ag−Se angles are between 104.81(6)° and 112.54(5)°. Similar highly distorted silver coordination geometries have also been observed in β-Ag_3AsSe_3 (Ag−Se distances, 2.651(6)−2.939(7) Å; Se−Ag−Se angles, 72.8(3)°−124.3(3)°).[21] Such a distortion is due to the packing necessities rather than the result of any significant $d^{10}\cdots d^{10}$ interactions, judging from the Ag···Ag contacts of 3.068(3) Å. A comparable Ag···Ag contact (3.006(7) Å) was found in

(21) Kanatzidis, M. G.; Chou J.-H. *J. Solid State Chem.* **1996**, *127*, 186−201.

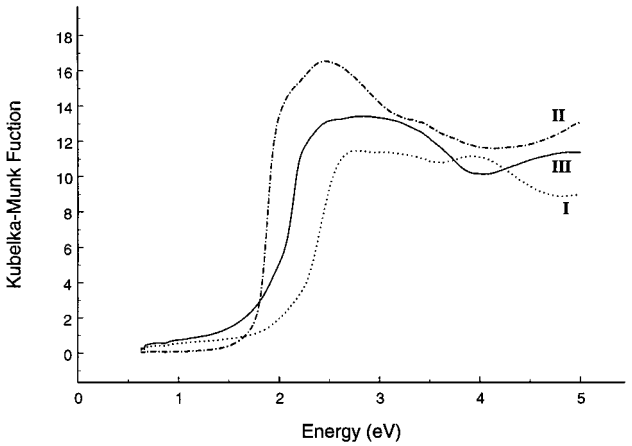

Figure 5. Optical absorption spectra of $K_2MnSn_2Se_6$ (**I**), $K_2MnSnSe_4$ (**II**), and $K_2Ag_2SnSe_4$ (**III**).

$K_2Ag_2SnTe_4$, which has a completely different 3D channel structure formed by corner- and edge-sharing $SnTe_4$ and $AgTe_4$ tetrahedra, although it has the same $K_2Ag_2SnQ_4$ stoichiometry.[4] $K_2Ag_2SnTe_4$ also differs from $K_2MnSnSe_4$ described above in that it features the octagonal-shaped tunnels and both of the crystallographically independent silver atoms are disordered. The two shortest interlayer Se···Se contacts in $K_2Ag_2SnSe_4$ are 3.713(3) (Se1−Se1) and 3.726(3) Å (Se2−Se2), again beyond the Se−Se bonding range.

Physical Properties. Thermal analysis via DSC indicated that $K_2MnSn_2Se_6$ (**I**) is stable up to 590 °C (the upper limit of our equipment). $K_2MnSnSe_4$ (**II**) showed a single endotherm at about 243 °C upon heating. The XRD patterns of its DSC residues revealed the presence of elemental selenium and other unknown phases, the decomposition products of **II**. $K_2Ag_2SnSe_4$ (**III**) was found to congruently melt at about 510 °C.

All three title compounds are electron precise and are predicted to be semiconductors. The optical properties were examined by analyzing their diffuse reflectance data. The Kubelka−Munk functions[8] for **I**, **II**, and **III** were converted from the diffuse reflectance data ($F = (1 - R_\infty)^2/2R_\infty$, where R_∞ is the relative diffuse reflectance of an infinitely thick layer; for practical purposes, this can be achieved at a layer depth of a few millimeters). Plotted in Figure 5 are remission functions versus the wavelength. The spectra of all three compounds display steep absorption edges, confirming the expected semiconducting nature. The optical band gaps obtained by extrapolation of the linear portion of the absorption edges are roughly 2.0 eV (**I**), 1.7 eV (**II**), and 1.8 eV (**III**), respectively, which are consistent with the observed colors.

Acknowledgment. Financial support from the National Science Foundation (Grant DMR-9553066) is greatly appreciated. The TGA/DSC analyzer was purchased through an NSF ARI grant (CHE 9601710-ARI). H.-Y. Guo also acknowledges partial support from NNSFC (Grant 29673004).

Supporting Information Available: Tables of detailed crystallographic data, atomic coordinates of all atoms, isotropic and anisotropic thermal parameters, bond distances and angles, and ORTEP drawings for compounds **I**−**III** (PDF). Ordering information and instructions for Internet access is given on any current masthead page. This material is available free of charge via the Internet at http://pubs.acs.org.

CM0000447